Educational Administration: Theory and Practice
2023, 29(4), 1300-1307
ISSN: 2148-2403
https://kuey.net/ **Research Article**

Enhancing Aluminum Additive Manufacturing Quality Through Optimized Cycle Boundaries And ANN Modeling Of Laser Energy Distribution

Madhurima Kalluru[1*], Dr. Devaki Devi K[2]

[1*]Research scholar of JNTUA, Mechanical Department, GPREC Research Centre, Kurnool, AP, India,
E-mail: madhurima5012@gmail.com
[2]Associate Professor, Mechanical Department, GPREC, Kurnool, AP, India. E-mail: devakidevik.me@gprec.ac.in

***Corresponding Author:** Madhurima Kalluru
*Research scholar of JNTUA, Mechanical Department, GPREC Research Centre, Kurnool, AP, India,
E-mail: madhurima5012@gmail.com

Citation: Madhurima Kalluru. et al (2023). Enhancing Aluminum Additive Manufacturing Quality Through Optimized Cycle Boundaries And ANN Modeling Of Laser Energy Distribution, *Educational Administration: Theory and Practice*, 29(4), 1300-1307.
Doi: 10.53555/kuey.v29i4.1822

ARTICLE INFO

ABSTRACT

Metal powder can be used in additive manufacturing, especially with methods such as Selective Laser Melting (SLM), to create intricate metallic components. Optimising process parameters, sometimes referred to as cycle limits, such as laser power, speed, hatching distance, and layer thickness, is crucial to producing high-quality produced products. A lot of the final parts' mechanical qualities come from changing these parameters. An Artificial Neural Network (ANN) model that makes use of the Levenberg-Marquardt learning method has been used to tackle this optimization challenge. The tangent sigmoid function, which is easily implemented using MATLAB, is used as the activation function in the training and testing phases of the ANN. The primary material utilised in this experiment is powdered aluminum metal. The conventional mechanical attributes have been replaced with output metrics including Volumetric Energy Density (VED), Surface Energy Density (SED), and Linear Energy Density (LED). A structural integrity and functional assessment is eventually impacted by these factors, which shed light on energy distribution and fusion characteristics during the SLM process. Measuring the difference between expected and actual outcomes, the Mean Square Error (MSE), must be minimized by optimizing cycle boundaries. Further evaluating the prediction accuracy of the ANN model is the correlation coefficient (R^2). This work intends to push quality and control in aluminum additive manufacturing forward more quickly with SLM. In conjunction with ANN-based modelling, this is accomplished by deliberately altering cycle boundaries based on LED, SED, and VED properties. Researchers hope to improve outcomes in aluminum additive manufacturing by better understanding and controlling the SLM process through the integration of various technologies.

Keywords: Additive manufacturing, Aluminum Metal powder, Artificial Neural Network, and Levenberg-Marquardt Algorithm.

1.INTRODUCTION

After moving beyond its roots in rapid prototyping, additive manufacturing (AM) has become a significant participant in the manufacturing sector during the past ten years. The process of producing products layer by layer from 3D model data is known as additive manufacturing (AM), and it represents a creative break from conventional subtractive manufacturing techniques (ASTM - F2792). [1][2][3].

Due to its multiple potential benefits, this technology has attracted considerable attention from a variety of industries, including aviation, biomedicine, and the automotive. These advantages include more adaptability to a range of materials, faster product development, less material waste, lighter components, and enhanced design freedom. [4][5][6][7]. Selective Laser Melting (SLM) stands out among the variety of AM techniques as the best technology for creating delicate metallic parts by totally melting metal powder, a feat unfeasible by

traditional subtractive procedures. [8][9][10][11].
It is commonly acknowledged that certain process variables, including laser power, scan speed, layer height and hatch spacing, have a significant impact on the ultimate quality and robustness of made products. The final product's overall quality and durability can be greatly improved by achieving the ideal combination of these factors [12][13]. With laser power indicating the amount of energy transferred per second and scan speed dictating the amount of time spent on a single location, the interaction between scan speed and laser power has significant significance. The relationship between these numbers determines how much energy is applied there [14].

Another crucial element, hatch spacing, affects how the laser beam's energy is distributed. While decreasing hatch spacing results in track overlap and potential problems with neighboring laser tracks, increasing hatch spacing focuses less energy toward the outer zone of the laser beam track. To maximize output while ensuring optimum powder melting, the right hatch spacing must be chosen [15]. The resolution of a part is substantially impacted by layer height. For high-resolution printing and to avoid structural flaws, the proper balance must be struck between maximizing height and maintaining layer adhesion [16]. The quality of the finished product is significantly influenced by these particular parameter values. As a result, improving the strength and overall quality of the finished product still depends on finding the perfect balance between these process boundaries [17][18].

Numerous forecasting methods and models have been developed in the field of additive manufacturing to choose the best parameter combinations. Artificial Neural Network (ANN) models have been popular among these strategies as prediction tools for enhancing cycle boundaries across various materials and manufacturing processes. When dealing with dynamic input cycle boundaries, ANN models excel in predicting parameter connections [19][20][21]. Researchers have investigated the impact of SLM cycle borders on microstructure and thermomechanical reactions in parts manufactured using AM, such as Saedi et al. These studies emphasize how important it is to carefully choose cycle boundaries to provide different features and behaviors in the manufactured components [22]. Additionally, employing a similar modeling strategy, Mehrpouya et al. employed ANN models to determine the ideal laser settings for NiTi components, finding a good correlation between the input parameters and projected values [23].

1.1. Parameters for input

When executing an SLM procedure, a number of parameters need to be adjusted. These elements are critical and have the ability to significantly alter the quality of the result. A thorough understanding of these process features is necessary for both energy optimization and effective model training. Four important parameters are selected as the inputs for our model. A more thorough explanation of these parameters may be found below: Layer thickness, hatching distance, laser power, and scan speed [25].

Laser Power: The energy absorbed during powder melting is determined by laser power, which makes it essential. Uneven melting of the powder due to improper calibration or overly high power can cause defects and porosity. On the other hand, overpowering could prevent heat from dissipating and result in over burning. Generally speaking, SLM apparatus uses 200–1,000 W power lasers.

Scan Speed: During SLM sintering, scan speed is crucial. Quicker scan rates reduce the size of the molten pools, changing their flow and the quality of the finished product. On the other hand, dropping too fast could cause droplets to splash and result in microstructural abnormalities. To get a uniform, cemented structure, the right scan speed must be used.
Hatch Distance: Hatch Distance impacts density and surface quality in SLM fabrication. It's the distance a laser route takes. Scan times are accelerated by a greater distance, but thicker layers require modification. A range of 0.05 to 0.25 mm is excellent.
Layer Thickness**:** Layer Thickness in additive manufacturing controls surface polish and product quality. While thicker layers speed up printing but may lose detail, thinner layers provide smoothness and detail but may slow down printing. Application, material, and machine capabilities all influence the decision, which usually ranges from 0.02 to 0.1 mm.

$$B = h \cdot t \cdot v \qquad (1)$$

1.2. Output Parameters :

When developing a construction task, a number of parameters are set at the job's inception and added to the program's parameter set. Prior to integrating the previously given parameters, critical parameters need to be computed [26].
Linear Energy Density (LED):
For evaluating the energy input into the powder bed, LED is essential. It is represented in J/mm and is computed by dividing the power by the scanning speed.

$$LED = P/V \qquad (2)$$

Surface Energy Density (SED):
Secondly, hatching distance divided by LED yields SED, which is another crucial element. It represents the energy that the laser beam applies to the surface and is given in J/mm^2.
SED = P/V*H (3)
Volume Energy Density (VED):
An essential component of a successful construction job design is VED, which is the power that the laser beam delivers to the working volume. It is calculated by dividing SED by the layer height, which needs to be determined in advance, and is represented in J/mm^3
VED = P/V*H*T (4)

2. Artificial Neural Networks Methodology (ANN)

Recent years have seen a substantial increase in the study of artificial intelligence (AI), which has found use in several fields, including computing, engineering, statistics, and the physical and mathematical sciences. In this AI world, artificial neural networks (ANNs), which can learn and adapt to their surroundings, have become potent tools. They are exceptional at solving pattern recognition, data categorization, and application-specific problems that are frequently challenging to solve using traditional methods [24][25][26]. In this study, the Multi-Layer Perception (MLP) neural network model and techniques, most notably the feed-forward back propagation algorithm, are used in conjunction with the MATLAB toolset. These resources are used to develop precise predictive models. The toolkit makes use of core elements like activation functions and different learning techniques, which may be tailored to the user's needs to ensure that the model is properly analyzed and the code is performed with the fewest restrictions possible.
The input layer,hidden layer and output layer are the three layers that makeup the MLP neural network architecture. The input received and the weights given to connections between input items and hidden neurons determine each hidden neuron's function. All hidden neurons must be active for these weights to be computed, therefore changing them will change how the hidden layer is represented. The network's connections between neurons are crucial in determining how well the system works.
The MLP model is similar to gradient descent (GD) training functions with adaptive learning rates in function estimation since it frequently incorporates the back-propagation (BP) algorithm. These methods incrementally change the weight and bias settings to reduce the discrepancy between the network's predictions and the actual results. An input layer, a hidden layer with a predetermined number of hidden neurons (in this instance 10,) and an output layer normally make up a network architecture. Cycle boundaries, which in this case include variables like laser power, scan speed, layer height, and hatch spacing, make up the input layer. Figure 1's illustration of the ANN modeling method shows how these parameters are utilized to estimate the ultimate tensile strength, which is used as the output layer.

Table 1: Experimental Observations

R	A	B	C	D	R1	R2	R3
1	325	1100	0.25	0.03	0.29	14.77	39.39
2	295	1300	0.12	0.06	0.22	3.8	30.05
3	317	1000	0.25	0.04	0.31	7.93	32.01
4	370	900	0.17	0.04	0.41	10.28	79.05
5	370	1300	0.25	0.02	0.28	14.23	57.22
6	370	955	0.15	0.02	0.38	19.37	129.4
7	370	1270	0.15	0.05	0.29	5.83	31
8	314	900	0.19	0.06	0.34	5.81	30.89
9	295	1100	0.12	0.03	0.26	8.94	71.55
10	310	1270	0.25	0.05	0.24	4.88	16.7
11	325	1250	0.25	0.04	0.26	6.5	25.74
12	325	1300	0.15	0.03	0.25	8.33	56.05
13	370	1235	0.1	0.04	0.3	7.49	74.68
14	370	1300	0.25	0.02	0.28	14.2	56.02
15	370	1270	0.15	0.03	0.29	7.3	49.61

2.1. MLP Neural Network Model

The MLP neural network has three layers' inputs, hidden, and output. Hidden neurons' behavior is shaped by received data and connection weights. The energy density between input and hidden components is established when all hidden products are active. The hidden layer's behavior can be modified by adjusting the energy density between the input and hidden components. The effectiveness of the network is significantly influenced by how the neurons are connected. The MLP model often trains using the back-propagation aa(BP) method and uses gradient descent (GD) as a training function [26]. By modifying the data and bias values, this procedure seeks to reduce the discrepancy between the network's predictions and the original results. The network design consists of an input layer representing cycle boundaries (laser intensity, scanning rate, layer thicknesses, and inter-hatch distance) and an output layer representing LED, SED, and VED. Complex pattern recognition and feature extraction are facilitated by a hidden layer with 10 neurons between these layers. Neurons in each layer must be connected and communicate with one another for information to circulate and be processed in the network. As was indicated Previously, neurons in each layer would take weighted inputs from the layer below and pass them on to the layer above, outputs are the weighted input signal sum, and the nonlinearity and complexity in the equation transmit that sum in Equation 6. Equation 7 was used to calculate the network error in MSE. Considering the relationship between the expected and actual results. In most cases, the preparation cycle continues, but this inaccuracy still achieves an acceptable result.

$$Y_{net} = \sum_{i=0}^{n} X_i w_i + w_0 \qquad (5)$$

$$Y = f\,(Y_{net}) = \frac{1}{1+e^{-y_{net}}} \qquad (6)$$

$$MSE = \frac{1}{k}\sum_{i=1}^{k} (Y_i - O_i)^2 \qquad (7)$$

$$\text{Var}\ (y) = E\ [(Y_i - E[Y])^2] \qquad (8)$$

$$R^2 = 1 - \frac{MSE}{var\ (y)} \qquad (9)$$

where the Y_i is neuron's response, f(Y_{net}) represents the activation function, Y_{net} is weighted input sum., X_i represents the input neurons ,w_i is the weight of coefficient, w_0 represents bias, MSE represents the mean square error between predicted and actual results, and O_i is actual value Sigmoid function is for testing/training. The correlation coefficient is expressed as E(Y) [26].Usually, we use equations 5,6,7,8 to calculate predicted values for inputs and output parameters. However, we can simplify the process by using the MATLAB toolkit.

3. Results and Discussions:

3.1 Predictive Modeling and Results for Additive Manufacturing Part Quality:

The cycle limits used in this study, such as layer power, scanning speed, hatching distance, and layer thickness, are input data. 15 datasets are randomly selected for modeling and split into 70% training, 15% validation, and 15% testing phases. The Levenberg-Marquardt algorithm is employed for model training and testing. The model is intended to predict optimal constraints for additive manufacturing patterns while focusing on achieving desired results.

This approach requires more memory but runs faster. When generalization stops developing, training comes to an end as evidenced by an increase in the validation samples' mean square error. The average squared discrepancy between outputs and objectives is defined as the mean squared error. Lower numbers are preferred. There is no error if the value is zero.

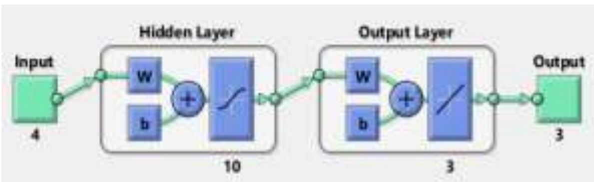

Fig. 1..The design of neural network input/output boundaries

The study focuses on constructing Artificial Neural Networks (ANNs) and analyzing their performance based on various factors such as ANN configuration, learning rules, and the number of hidden neurons. Metrics such as Mean Square Error (MSE) and correlation coefficient are applied to evaluate the performance of neural networks when working with training, validation, and testing datasets and by computing the MSE with equation 7.The study uses tables and graphs to display predicted values using ANN models, assessing the impact of input deviations on measured outputs.Training, Validation, and Testing lines are represented graphically in Table7 using different colours. While Mean Squared Error (MSE) and R values are computed using input and output data taken from the composite matrix within the Design of Experiments (DoE), these lines represent the relationship between samples. Fig 2 showcases a title window of the neural network during training, displaying progress and allowing interruption using a quit button.

Fig . 2. Training, Validation, and Testing Information for Samples

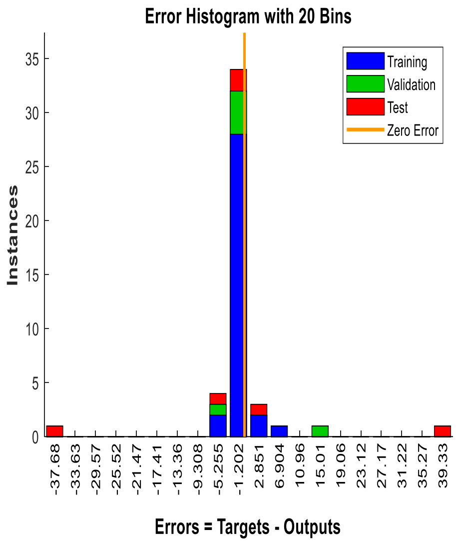

Fig 3.(a)Training error using histogram

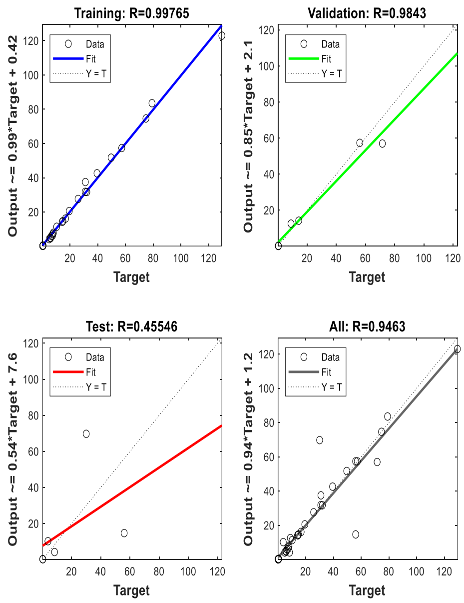

Fig (b)Regression during the training period

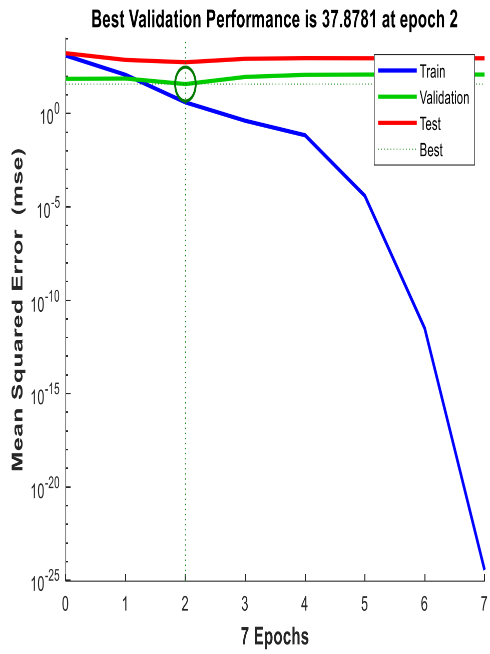

Fig (c) Training performance

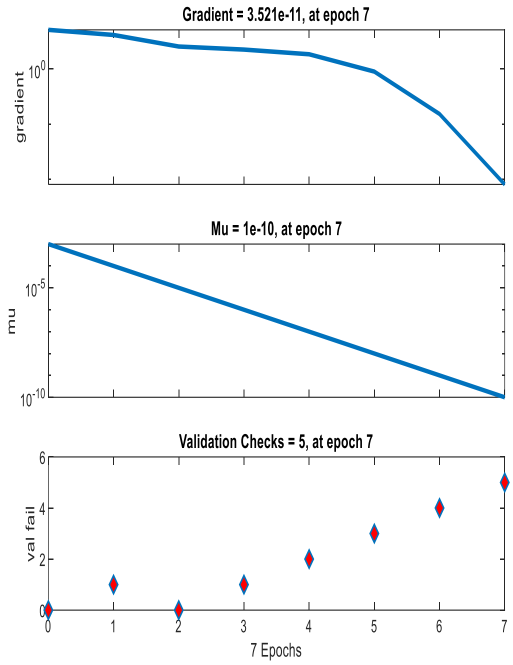

Fig (d) Gradient descent

The explanatory window of neural network (NN) training performance is displayed in Fig b. The best validation performance, which demonstrates the best mean squared error (MSE) combination, is seen at epoch 2 at 37.87. Fig d. shows the neural network performs best when the outcomes of training, validating, and testing are combined. The "training histogram" is a visual representation of how frequently the network's educated guesses are incorrect. The ideal line that reduces errors throughout the training, validation, and testing phases exemplifies the efficiency of ANN models. Fig 3 shows how computing the gradient's loss function is employed in the context of learning back propagation to modify the weight of neurons. The valid check is 5 at epoch 7, and the gradient value is 68.7045%. For the normal period of 18 epochs, training is stopped if validation efficiency declines to prevent the training network from acting poorly during non-training. Various output patterns for testing (R = 0.8046), validation (R = 0.9888), and training (R = 0.9945) are displayed in Fig d. These ANN forecasts contribute to the overall response with an R-value of 0.8814, and the R^2 value was computed using equation 9. The relationship between the actual outcomes and those anticipated by the ANN is demonstrated by the regression plot in this figure. The ANN findings and the objective are in agreement. Since the R-value is 0.9463, there is a clear agreement between the ANN findings and the desired outcome. The link between desired an objective and realized results is precisely quantified by regression values.

Conclusion

In conclusion, this work emphasizes the crucial role that screening designs and Design of Experiments (DoE) play in resolving complex interactions between process variables, thereby increasing understanding and decision-making, particularly in the context of additive manufacturing. Notably, the study makes use of Artificial Neural Networks (ANN) to effectively combine complicated data and predict outcomes, obtaining an astonishing 94.63% alignment with real results during validation. Importantly, this research's ramifications go beyond selective laser melting (SLM), providing helpful information for a variety of production processes. This research has the potential to transform processes and improve product quality across industries through the integration of DoE, ANN modeling, and quality prediction. The significance of systematic experimentation and predictive modeling as drivers of improvements in manufacturing and process optimization's is shown by these findings.

Acknowledgment:

The reviewers, who remained anonymous, have our sincere appreciation for their insightful comments.

Data Availability:

We declare that every piece of information contained in this manuscript is unique and does not come from outside sources.

Conflict of Interest:
There are no conflicts of interest involving this work, according to the authors.

Ethics Approval:
The authors claim that the reported study was not impacted by any conflicting financial or personal interests.

Consent to Participate:
All authors freely contributed to this study project with their own free will.

Consent for Publication:
The authors give the journal their consent to publish this study.

REFERENCES

[1] Abdelhamid O, Al-Ahmar A, Ameen W and Mian S H 2019 Additive manufacturing: challenges, trends, and applications Adv. Mech. Eng. 11 1–27

[2] Przyklenk A et al 2021 New European metrology network for advanced manufacturing Meas. Sci. Technol. 32 111001

[3] Ahmed N 2019 Direct metal fabrication in rapid prototyping: a review J. Manuf. Process. 42 167–91

[4] Hague R and Tuck C 2007 ATKINS: Manufacturing a low carbon footprint-zero emission enterprise feasibility study Loughborough University (Atkins) pp 1–24

[5] Bhardwaj T and Shukla M 2020 Laser additive manufacturing direct energy deposition of Ti-15Mo biomedical alloy: artificial neural network-based modeling of track dilution Lasers Manuf. Mater. Process.

[6] Ragab M and Sabir M F S 2022 Outlier detection with optimal hybrid deep learning enabled intrusion detection system for ubiquitous and smart environment Sustain. Energy Technol. Assess. 52 102311.

[7] Jacob G, Donmez A, Slotwinski J, and Moylan S 2016 Measurement of powder bed density in powder bed fusion additive manufacturing processes Meas. Sci. Technol. 27 115601 .

[8] Zhao X and Rosen D W 2017 Real-time interferometric monitoring and measuring of photopolymerization based stereolithographic additive manufacturing process: sensor model and algorithm Meas. Sci. Technol. 28 015001.

[9] Majeed A, Zhang Y, Lv J, Peng T, Atta Z and Ahmed A 2020 Investigation of T4 and T6 heat treatment influences on relative density and porosity of AlSi10Mg alloy components manufactured by SLM Comput. Ind. Eng. 139 106194

[10] Peng T, Lv J, Majeed A and Liang X 2021 An experimental investigation on energy-effective additive manufacturing of aluminum parts via process parameter selection J. Clean. Prod. 279 123609.

[11] Akshay Kumar, PL. Ramkumar, Aman Shukla, and Nikita Gupta, Prediction of Mechanical Properties in Rotational Moulding of LLDPE Using Machine Learning Model for the Given Oven Residence Time, https://link.springer.com/chapter/10.1007/978-981-33-4176-0_14.

[12] Somers M J and Casal J C 2008 Using artificial neural networks to model nonlinearity: the case of the job satisfaction—job performance relationship Organ. Res. Methods 12 403–17.

[13] Card S K, Moran TP and Newell A 2018 The Psychology Of Human-Computer Interaction (https://doi.org/10.1201/ 9780203736166) .

[14] Chowdhury S, Mhapsekar K and Anand S 2018 Part build orientation optimization and neural network-based geometry compensation for additive manufacturing process J. Manuf. Sci. Eng. Trans. ASME 140 1–29.

[15] Francesco Trevisan 1,2, Flaviana Calignano 2, Massimo Lorusso 2, Jukka Pakkanen 1,2, Alberta Aversa 1, Elisa Paola Ambrosio 2, Mariangela Lombardi 1, Paolo Fino 1,2 and Diego Manfredi 2,On the Selective Laser Melting (SLM) of the AlSi10Mg Alloy: Process, Microstructure, and Mechanical Properties, Materials 2017, 10, 76; doi:10.3390/ma10010076.

[16] Ding D, Pan Z, Cuiuri D, Li H, van Duin S and Larkin N 2016 Bead modeling and implementation of adaptive MAT path in wire and arc additive manufacturing Robot. Comput.-Integr. Manuf. 39 32–42.

[17] Ding D, Shen C, Pan Z, Cuiuri D, Li H, Larkin N and van Duin S 2016 Towards an automated robotic arc-welding-based additive manufacturing system from CAD to finished part Comput.-Aided Des. 73 66–75

[18] Mehrpouya M, Gisario A, Huang H, Rahimzadeh A and Elahinia M 2019 Numerical study for prediction of optimum operational parameters in laser welding of NiTi alloy Opt. Laser Technol. 118 159–69.

[19] Mehrpouya M, Gisario A, Rahimzadeh A, Nematollahi M, Baghbaderani K S and Elahinia M 2019 A prediction model for finding the optimal laser parameters in additive manufacturing of NiTi shape memory alloy Int. J. Adv. Manuf. Technol. 105 4691–9.

[20] Nelson J. C., Xue S., Barlow J. W, Beaman J J, Marcus H L, and Bourell D L 2002 Model of the selective laser sintering of bisphenol-A polycarbonate Ind. Eng. Chem. Res. 32 2305–17.

[21] Yardimci M A, Guceri S I and Danforth S C 1995 A phenomenological numerical model for fused deposition processing of particle-filled parts 1995 Int. Solid Freeform Fabrication Symp. (https://doi.org/10.15781/T2NV99W2B).
[22] Trevisan F, Calignano F, Lorusso M, Pakkanen J, Aversa A, Ambrosio E, Lombardi M, Fino P and Manfredi D 2017 On the selective laser melting (SLM) of the AlSi10Mg alloy: process, microstructure, and mechanical properties Materials 10 76 .
[23] Gupta A K, Lloyd D J and Court S A 2001 Precipitation hardening in Al-Mg-Si alloys with and without excess Si Mater. Sci. Eng. A 316 1–2.
[24] SEVIMEC, EL PROCESO DE MECANIZADO. [https://sevimec.es/es/el-proceso-demecanizado, January 12, 2017].
[25] Kumar S 2014 Selective laser sintering/melting Comprehensive Mater. Process. 10 93–134
[26] Qiu C, Panwisawas C, Ward M, Basoalto H C, Brooks J W and Attallah M M 2015 On the role of melt flow into the surface structure and porosity development during selective laser melting Acta Mater. 96 72–79.